Journal of CO2 Utilization 94 (2025) 103060

Contents lists available at ScienceDirect

Journal of CO2 Utilization

journal homepage: www.elsevier.com/locate/jcou

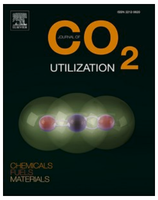

Utilization of carbon dioxide and nitrate to produce sodium bicarbonate through a nitrate hydrogenation method

Hee Sun Park [a,1], Jae Yeon Kim [a,1], Hee Jung Yang [a], Youlim Chung [b,c], Jonggeol Na [b,c,*], Nam Hwi Hur [a,**]

[a] Department of Chemistry, Sogang University, Seoul 04107, Republic of Korea
[b] Department of Chemical Engineering and Materials Science, Ewha Womans University, Seoul 03760, Republic of Korea
[c] Graduate Program in System Health Science and Engineering, Ewha Womans University, Seoul 03760, Republic of Korea

ARTICLE INFO

Keywords:
Nitrate hydrogenation
Hydrogen-bearing oxide catalyst
Catalytic synthesis
CO_2 utilization
Soda ash

ABSTRACT

Sodium carbonate (Na_2CO_3), known as soda ash, is used in various industrial processes such as glass making, detergent, metallurgy, and water treatment, which is produced from salt brine (NaCl) and limestone ($CaCO_3$) in the presence of ammonia by the Solvay process. Although the Solvay process is fully optimized, it requires large amounts of energy, generates significant CO_2 emissions, and produces undesirable byproducts. Here we describe a catalytic strategy that can address the energy and environmental challenges facing the Solvay process. The hydrogen-bearing H_xRuO_2 catalyst selectively hydrogenates nitrate to ammonia, facilitating the conversion of CO_2 into sodium bicarbonate ($NaHCO_3$) through mineralization and yielding valuable ammonium bicarbonate (NH_4HCO_3). We also report on the techno economic analysis and life cycle assessment of the catalytic process compared to the Solvay process via rigorous commercial-scale process design and thereby propose a clear solution to mitigating CO_2 emission, reducing energy consumption, and alleviating the environmental threat without loss of economic feasibility. The newly developed catalytic route might offer a promising alternative process to produce soda ash via an atom economic synthetic route.

1. Introduction

Soda ash (Na_2CO_3) is an essential chemical raw material with a global annual production volume of over 65 million tons in 2023 [1]. The Solvay process, which is the most widely used production method, accounts for approximately 45 % of global production capacity [2]. The Hou process, which is very similar to the Solvay process, uses sodium chloride, carbon dioxide, ammonia, and water as starting materials and represents about 25 % of global production capacity [3]. However, the Hou process is more energy-intensive than the Solvay process, which requires about 14.25 GJ of energy per tonne of Na_2CO_3. In contrast, the Trona process, based on trona deposits, is less energy-intensive, requiring about 5.6–7 GJ per tonne of Na_2CO_3 and represents 23 % of global production capacity [2]. Despite its lower energy requirements, the Trona process is not sustainable due to the limited availability of high purity trona deposits. Unlike the Hou and Trona processes, the Solvay process uses readily available inexpensive brine (NaCl) and limestone ($CaCO_3$) as sources of sodium and carbonate ions, respectively. The reaction between brine and limestone, given by $2NaCl + CaCO_3 \rightarrow Na_2CO_3 + CaCl_2$, seems straightforward, but does not proceed without ammonia. Moreover, a large amount of energy is required to obtain CaO and CO_2 from the calcination of $CaCO_3$ above 825 °C. Worse than this energy-intensive process, the Solvay process generates enormous amounts of chemical wastes, including $CaCl_2$-laden wastewater and brine purification sludge, which exceeds the capacity of conventional disposal sites and is consequently dumped into rivers or seawater [4].

Several modifications to the Solvay process have been investigated to produce soda ash via environmentally benign and economical routes [5–15]. Wu and coworkers reported a novel proton cycled membrane electrolysis (PCME) technique to make sodium carbonate with low energy consumption. Compared with the Solvay process, the energy consumption is reduced by about 60.9 %, but the CO_2 absorption rate is considerably lower in the PCME process [16]. Forster provided

---

* Corresponding author at: Department of Chemical Engineering and Materials Science, Ewha Womans University, Seoul 03760, Republic of Korea.
** Corresponding author.
E-mail addresses: jgna@ewha.ac.kr (J. Na), nhhur@sogang.ac.kr (N.H. Hur).
[1] These authors contributed equally to this work.

https://doi.org/10.1016/j.jcou.2025.103060
Received 10 November 2024; Received in revised form 23 January 2025; Accepted 7 March 2025

theoretical and experimental data demonstrating the feasibility of a $MgCl_2/MgO$-modified ammonia soda process in which Na_2CO_3 and HCl are produced from CO_2, NaCl, and H_2O [17]. The modified process to produce sodium carbonate might be promising because it could utilize the emitted CO_2 gas and completely avoid the formation of $CaCl_2$ as a by-product. However, the downside of this method is that temperatures above 800 K are required to operate the modified ammonia soda process. Dual process, developed by Asahi chemical industry, uses NaCl, CO_2, and NH_3 as raw materials, which produces both sodium carbonate and ammonium chloride [18]. This reaction can be described as the following reaction: $NaCl + NH_3 + CO_2 + H_2O \rightarrow NaHCO_3 + NH_4Cl$. A notable merit is that by-products such as $CaCl_2$ are not produced, but the process has several engineering challenges, including difficult purification of brine, severe corrosion from ammonium chloride solution, and high refrigeration costs. Very recently, Hanein and coworkers proposed a low-temperature process in which $CaCO_3$ reacts directly with an aqueous solution of NaOH to produce $Ca(OH)_2$ and Na_2CO_3 [19]. This decarbonization method is expected to significantly reduce CO_2 emissions by combining the two lime and sodium carbonate manufacturing processes into one process. Further development of separation technologies and energy-efficient NaOH production processes is required to make this decarbonization process viable. Despite these advances, there is still no alternative method comparable to the improved Solvay process.

In the Solvay process, ammonia (NH_3) is crucial for facilitating the reaction of CO_2 with sodium chloride (NaCl) to produce sodium bicarbonate ($NaHCO_3$) and ammonium chloride (NH_4Cl). Ammonia is essential for promoting the carbonation reaction, as the reaction between CO_2 and NaCl does not occur in its absence. It is well known that ammonia can be generated through the thermal or electrochemical reduction of nitrate [20–28]. We envisioned that this nitrate hydrogenation method could be applied to the sustainable synthesis of sodium bicarbonate ($NaHCO_3$) from nitrate and carbon dioxide (CO_2). We have put more emphasis on the synthetic pathway without generating any byproducts. In this context, we selected sodium nitrate ($NaNO_3$) as a model precursor, as it supplies both sodium and nitrate sources. During the catalytic process, nitrate is converted to ammonia via hydrogenation. This ammonia then creates an alkaline environment, facilitating the mineralization of $NaHCO_3$ and ammonium bicarbonate (NH_4HCO_3). This approach could address some challenges associated with the traditional Solvay process.

Here we report an unprecedented catalytic strategy that can coproduce $NaHCO_3$ and NH_3 from $NaNO_3$ over a hydrogen-bearing ruthenium oxide (H_xRuO_2). In contrast to the Solvay process that involves multi-step reactions, this catalytic route is a one-pot reaction and does not produce any byproducts. Nearly complete conversion of $NaNO_3$ into $NaHCO_3$ and NH_4HCO_3 has been achieved in the catalytic reduction of $NaNO_3$ in the presence of CO_2 within a couple of hours. This newly discovered catalytic approach not only can utilize the emitted CO_2 but also can produce valuable chemicals such as $NaHCO_3$ and NH_3 in a nearly atom economical route, which can play an important role in mitigating global warming.

2. Experimental procedures

2.1. Materials and chemicals

All the chemicals were obtained from commercial suppliers and used without further purification unless otherwise stated. Anhydrous ruthenium dioxide (RuO_2) powder was purchased from Pressure Chemical Co. (Pittsburgh, PA, USA). Sodium nitrate ($NaNO_3$) and formic acid (HCOOH) were purchased from Sigma-Aldrich (Burlington, MA, USA). Carbon dioxide (CO_2, 99.999 %) and hydrogen (H_2, 99.99 %) gases were purchased from Donga Industrial Gas (Seoul, South Korea).

2.2. Characterization methods

Powder X-ray diffraction (XRD) spectra were recorded with a Rigaku Miniflex 600 diffractometer (Rigaku Mechatronics Co., Ltd., Japan) with Cu Kα radiation ($\lambda = 1.5406$ Å), operated at 40 kV and 15 mA. Samples were scanned at a rate of $20^\circ\ min^{-1}$ with a scan width of 0.02°. Ultraviolet-visible (UV–vis) spectra were measured using a Jasco V-660 spectrophotometer (Jasco, Inc., Japan) in the 200–500 nm region with 1 nm intervals. Solution pH was measured with an HI 5521 pH meter (Hanna Instruments, Inc., Italy). Field emission scanning electron microscopy (FE-SEM) was performed using a JSM-7100F (JEOL Ltd., Japan) with an X-Max EDS detector (Oxford Instruments, UK) for elemental analysis. Gaseous products were analyzed by gas chromatography Acme 6100 GC (Youngin Chromass Co., Ltd., South Korea) using a TCD detector with a Porapak N packed column.

2.3. Synthesis of H_xRuO_2

The H_xRuO_2 catalyst was synthesized using procedures similar to those in our previous publication [29], with formic acid as the starting reagent. Initially, 0.10 g of polycrystalline RuO_2 powder was placed in a 10 mL reaction vial, which was then immersed in a solution of 0.2 mL of formic acid and 0.2 mL of deionized water. This vial was transferred to a 45 mL stainless steel pressure reactor, which was pressurized to 5 bar of H_2 at room temperature. The reactor was then heated to 110 °C and maintained at this temperature for 12 hours. After the reaction, the reactor was allowed to cool to room temperature. The resulting black solid product was washed three times with ethanol and dried under vacuum for 2 hours.

2.4. Catalytic hydrogenation

The hydrogenation and carbonation reaction were conducted in a stainless-steel pressure reactor. Initially, a sodium nitrate solution of appropriate concentration was prepared by dissolving $NaNO_3$ powder in deionized water. The H_xRuO_2 catalyst (typically 20 mg) was immersed in this aqueous solution, which was then placed in a glass-lined 45 mL stainless steel pressure vessel equipped with a pressure gauge. The reactor was purged three times with 5 bar of H_2 and subsequently pressurized with H_2 (10–40 bar) and CO_2 (5–15 bar). Stirring was achieved using a magnetic stirrer, maintaining the reaction temperature within the range of 30–120 °C. After a specified reaction period, the reactor was cooled to room temperature.

The reaction product was separated into supernatant and precipitate through distillation (Scheme 1). The precipitate, composed of sodium-containing compounds such as desirable $NaHCO_3$ and unreacted $NaNO_3$, was washed with over 30 mL of water. The resulting suspension was then centrifuged to isolate water-soluble sodium compounds and the used catalyst. The sodium compounds obtained were recrystallized by evaporation and meticulously weighed to determine the yield. Diluted sulfuric acid was added to the supernatant solution containing ammonia species, which was subsequently evaporated to produce ammonium bisulfate (NH_4HSO_4). The remaining nitrate ions were quantified by measuring the absorption intensity in UV–vis spectra at 303 nm.

2.5. Recycling test

To evaluate the recyclability of the H_xRuO_2 catalyst, a series of experiments were conducted as follows: Initially, 20 mg of H_xRuO_2 catalyst was mixed with a $NaNO_3$ aqueous solution in a glass-lined 45 mL stainless steel pressure reactor. After purging the reactor twice with H_2 at room temperature, it was pressurized with 20 bar of H_2 and 5 bar of CO_2. The reaction temperature was maintained at 100 °C for 3 hours to ensure complete reaction, followed by cooling to room temperature. The resulting product was washed with water, and the supernatant

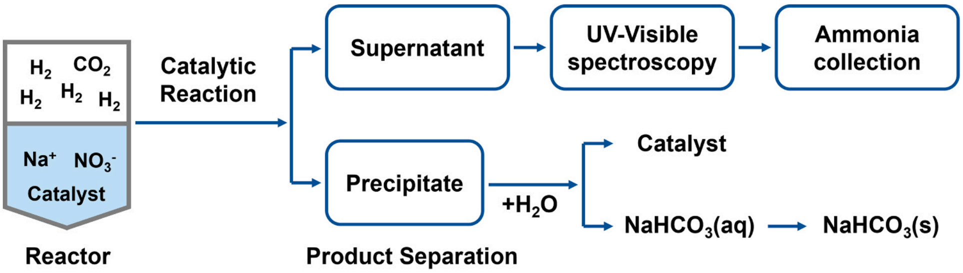

Scheme 1. Schematic illustrating the separation and analysis of reaction products.

containing sodium compounds was carefully separated from the H_xRuO_2 catalyst. The sodium compounds obtained were recrystallized by evaporation and characterized using UV–vis spectra and powder XRD. The yield of sodium compounds was determined gravimetrically. This catalytic reaction was repeated ten times under identical conditions using the recycled H_xRuO_2 catalyst.

2.6. Techno economic analysis (TEA)

We evaluated the net present value (NPV) and minimum selling price (MSP) based on cash flow to analyze the profitability of the process. The total capital investment (C_{TCI}) includes the total depreciable capital (C_{TDC}) and working capital (C_{WC}). The production cost, excluding depreciation ($C_{Excl.Dep}$), encompasses feedstock, utilities, maintenance, labor, operating overheads, insurance, and other expenses. C_{TCI}, as well as the utilities and feedstocks required for the process, were calculated using the process simulator Aspen Plus V12, with cost-related parameters sourced from Seider et al. [30]. The simulation thermodynamics method used is ENRTL-RK, which estimates thermodynamic data for electrolyte systems (e.g., salt formation, equilibrium reactions) [31,32]. The global chemical reactions considered in the process are detailed in Table S1 and incorporated into the model. Depreciation (C_D) is accounted for using a 7-year Modified Accelerated Cost Recovery System (MACRS). The plant life (N_{life}) is set at 25 years, including a 2-year construction period. Relevant economic indicators are calculated using Eqs. (1)-(3), with the MSP determined as the product cost when the final NPV reaches zero. Additionally, we analyzed how the economic potential of the process could be improved by adjusting cost parameters. Specifically, we varied the costs of sodium nitrate ($NaNO_3$) and hydrogen (H_2). For green hydrogen, we adjusted the cost to \$1.5/kg, assuming large-scale expansion of electrolyzers and cost reductions, with the base condition set at \$4.28/kg [33,34]. Similarly, the $NaNO_3$ price was adjusted to \$0.325/kg, assuming low-cost extraction from Chilean mines, with the base condition set at \$0.65/kg [35]. Detailed cost parameters and cash flow information are provided in the Supplementary Information (Tables S3 and S6).

$$\text{Net earnings (NE)}= (\text{Sales-}C_{Excl.Dep}\text{-}C_D) \times (1.0\text{-}t_{income}) \quad (1)$$

$$\text{Annual cash flow (CF)}= (\text{NE}+C_D)\text{-}C_{TDI} \quad (2)$$

$$NPV = \sum_{n=1}^{N_{life}} \frac{CF_n}{(1+i)^n} \quad (3)$$

2.7. Life cycle assessment (LCA)

We conducted a life cycle assessment to compare the environmental impacts of the Solvay process and the catalytic process. The data for the Solvay process are not derived from the Aspen simulations. The Solvay process was evaluated using average data from the literature [36]. A cradle-to-gate approach was applied, with the functional unit defined as the production of 1 ton of dense soda ash (Na_2CO_3). To ensure a fair comparison, the sources for common utilities used in both processes (e.g., steam, electricity, cooling water) were the same. The evaluation was carried out using SimaPro software, primarily utilizing the Ecoinvent v.3 database. For substances not included in the database, data were sourced from the literature [37]. The ReCiPe 2016 midpoint (H) method was used to calculate the Global Warming Impact (GWI), which measures the impact of greenhouse gas emissions on global warming. We assessed CO_2 emissions for the $NaNO_3$ production process under both base and optimal conditions. Under base conditions, CO_2 emissions from the mining and purification of sodium nitrate are included. For optimal conditions, it is assumed that CO_2 emissions are reduced by half (Table S6).

3. Results and discussion

3.1. Catalytic synthesis of sodium bicarbonate via nitrate hydrogenation

We have recently demonstrated an innovative metal extraction process from spent lithium-ion battery utilizing the selective hydrogenation of nitrate to ammonia. This catalytic method, based on the H_xRuO_2 catalyst, uses nitric acid (HNO_3), H_2, and CO_2 as starting materials, resulting in the production of metal values in the form of carbonates [38]. Our strategy for producing $NaHCO_3$ in a more sustainable manner leverages this nitrate hydrogenation technology. We use $NaNO_3$ and CO_2 as the initial reagents. $NaNO_3$ plays a dual role: it serves as a source for both sodium and nitrate. Meanwhile, carbon dioxide facilitates the conversion of sodium cations into insoluble $NaHCO_3$ through a carbonation/mineralization pathway. The H_xRuO_2 catalyst was chosen primarily for its exceptional stability in both acidic and alkaline solutions.

First, we assessed whether the H_xRuO_2 catalyst can convert $NaNO_3$ to $NaHCO_3$ through nitrate hydrogenation. All reactions were performed in a pressure reactor. The catalytic process begins by immersing $NaNO_3$ powder in an aqueous solution together with the H_xRuO_2 catalyst and then pressurizing it with H_2 and CO_2 gases. Initial screening experiments were conducted based on the following chemical reaction, denoted as Eq. (4).

$$NaNO_3 + 4H_2 + 2CO_2 \rightarrow NaHCO_3 + NH_4HCO_3 + H_2O \quad (4)$$

The stoichiometric reaction indicates a 1:4:2 ratio of $NaNO_3$:H_2:CO_2. However, under stoichiometric operation, $NaNO_3$ is not completely converted to $NaHCO_3$. Thus, H_2 and CO_2 gases were supplied in excess to ensure the full hydrogenation of all nitrate anions and complete carbonation of sodium and ammonium cations. To optimize the conditions for $NaHCO_3$ production, various factors such as temperature, reaction time, concentration, and the relative pressures of H_2 and CO_2 were evaluated. Table 1 summarizes the yields obtained under different conditions. The progress of the reaction and the products formed were carefully monitored using UV–visible spectroscopy and powder X-ray diffraction.

The reaction temperature gradually increased, starting from 30 °C. At 30 °C, a trace of $NaHCO_3$ was observed after 48 hours of reaction time. This result indicates that the hydrogenation of nitrate by the H_xRuO_2 catalyst proceeds very slowly at 30 °C. The powder X-ray diffraction (XRD) patterns of the products, depicted in Fig. 1a,

Table 1
Yield of $NaHCO_3$ produced from catalytic reactions of $NaNO_3$ under various conditions.

Entry	Temp (°C)	Time (h)	$NaNO_3$ (mmol)	Water (mL)	pH_2 (bar)	pCO_2 (bar)	Yield of $NaHCO_3$ (%)
1	30	48	4	1	20	5	10.42
2	50	2	4	1	20	5	15.32
3	60	2	4	1	20	5	24.21
4	70	2	4	1	20	5	28.38
5	80	2	4	1	20	5	53.83
6	100	2	4	1	20	5	> 99
7	120	2	4	1	20	5	> 99
8	100	2	4	1	10	5	14.29
9	100	2	4	1	15	10	57.03
10	100	2	4	1	10	15	14.67
11	100	2	4	1	40	10	> 99
12	100	2	4	4	20	5	80.68
13	100	2	4	2	20	5	54.52
14	100	2	4	0.5	20	5	29.11
15	100	5	8	1	40	10	> 99
16[a]	100	24	118.5	100	40	10	> 99

[a] The reaction was conducted in a 600 mL stainless steel pressure reactor.

demonstrate that the conversion of $NaNO_3$ to $NaHCO_3$ occurs more significantly at temperatures above 50 °C. The powder XRD data indicate that the yield of solid $NaHCO_3$ increased progressively with the reaction temperature, as shown in Fig. 1b. The formation of $NaHCO_3$ was much faster when the reaction was performed at 80 °C. Complete conversion is achieved at 100 °C within 2 hours. At 120 °C, $NaHCO_3$ is produced alongside small amounts of sodium carbonate monohydrate ($Na_2CO_3{\cdot}H_2O$), indicating that 100 °C is the optimal temperature for complete carbonation to $NaHCO_3$. Above 100 °C, $NaHCO_3$ begins to decompose into sodium carbonate (Na_2CO_3) and CO_2. Utilizing the temperature-dependent data and the Arrhenius equation, we determined the activation energy of the reaction. The Arrhenius plot is presented in Fig. S1, and the activation energy (E_a) is calculated to be 36.5 kJ/mol.

Analysis of products by powder XRD clearly shows the formation of $NaHCO_3$. This observation demonstrates that the catalytic reaction sequesters CO_2 in a desirable and stable mineral form. Additionally, the ammonia gas produced from nitrate hydrogenation reacts with excess CO_2 in an aqueous solution, yielding a significant amount of NH_4HCO_3 (Fig. 1c). Ammonium bicarbonate holds value as a feedstock for fertilizer. A remarkable feature is that all the reactants, including $NaNO_3$, H_2, and CO_2, are utilized to produce $NaHCO_3$ and NH_4HCO_3. This synthetic process consists of two primary reactions: one is the selective hydrogenation of nitrate to ammonia, and the other is the carbonation of sodium and ammonium cations. It is worth mentioning that this process is almost atom-economical, although a slight excess of H_2 and CO_2 gases is used to promote reaction. Unreacted H_2 and CO_2 gases can be recycled for use in subsequent reactions.

To evaluate the effect of the pressure ratio between H_2 and CO_2 on the formation of $NaHCO_3$, the total pressure was fixed at 25 bar. The experiment was performed by varying the pressure ratio. The $NaHCO_3$ yields from entry 8 to entry 10 in Table 1 were reduced (see also Fig. 2a), indicating that a H_2 to CO_2 ratio of 4:1 is optimal at a total pressure of

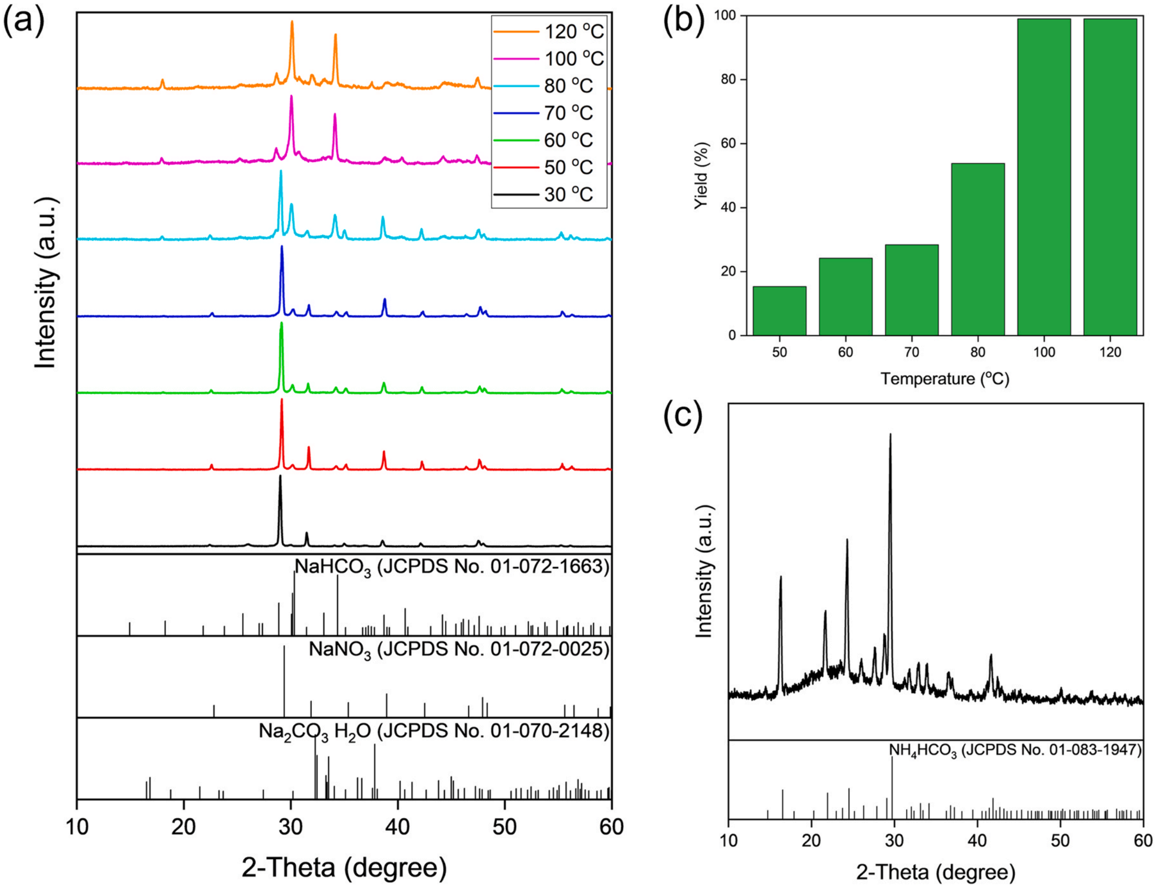

Fig. 1. (a) Powder X-ray diffraction (XRD) data of the reaction products synthesized at seven different temperatures under the following conditions: 20 mg of catalyst, 4 mmol of $NaNO_3$, 1 mL of water, 20 bar of H_2, 5 bar of CO_2. For 30 °C the reaction time is 48 hours, and for all other temperatures, the reaction time is 2 hours. The XRD patterns include reference entries from the Joint Committee on Powder Diffraction Standards (JCPDS) for $NaHCO_3$, $NaNO_3$, and $Na_2CO_3{\cdot}H_2O$ at the bottom. (b) Yields of $NaHCO_3$ at these six different temperatures. (c) Powder XRD pattern of NH_4HCO_3 obtained after reaction. JCPDS data of NH_4HCO_3 are shown in the bottom panel.

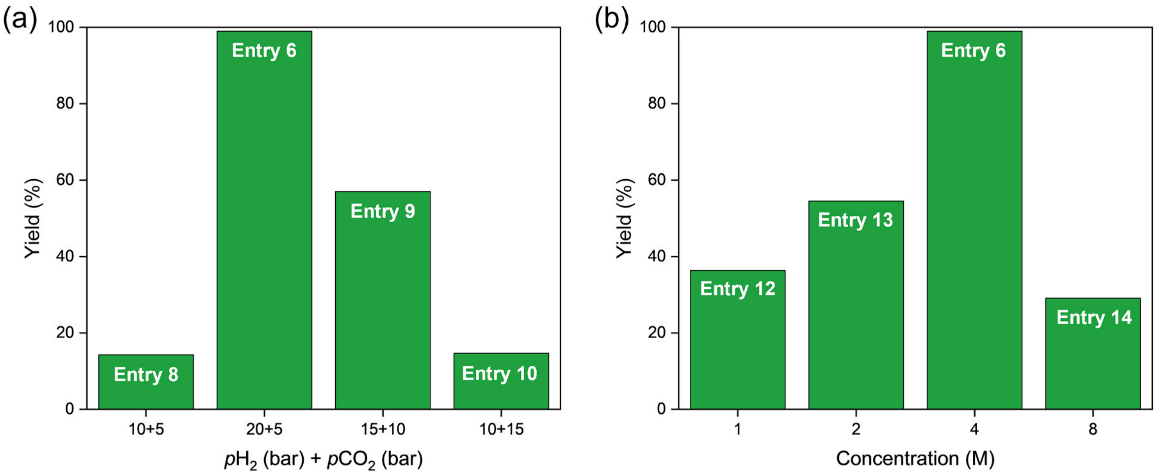

Fig. 2. (a) Evaluation of the effect of the pressure ratio between H_2 and CO_2 on the yield of $NaHCO_3$ under the following conditions: 20 mg of catalyst, 4 mmol of $NaNO_3$, 1 mL of water. The reactions were performed at 100 °C for 2 hours. In entry 8, the total pressure is 15 bar, and in the other entries, the total pressure is fixed at 25 bar. (b) Evaluation of the impact of $NaNO_3$ concentration on the yield of $NaHCO_3$ under the following conditions: 20 mg of catalyst, 4 mmol of $NaNO_3$, 20 bar of H_2, 5 bar of CO_2. The reactions were performed at 100 °C for 2 hours. The corresponding entry numbers in Table 1 are indicated within the rectangular bars.

25 bar. The molar amounts of H_2 and CO_2 gases used in entry 6 of Table 1 are 40 mmol and 10 mmol, respectively, which establishes a molar ratio of $NaNO_3$:H_2:CO_2 at 1:10:2.5. The highest yield is achieved at this 1:10:2.5 molar ratio of $NaNO_3$:H_2:CO_2 (entry 6, Table 1), suggesting that this is the optimal molar ratio. Compared to the stoichiometric equation presented in (4), the amount of H_2 used in entry 6 of Table 1 exceeds the stoichiometric requirement by a factor of 2.50, while the amount of CO_2 slightly exceeds it by a factor of 1.25. When the total pressure increased from 25 bars to 50 bars while maintaining the H_2 to CO_2 ratio at 4:1, the yield of $NaHCO_3$ remained over 99 % (entry 11, Table 1). This indicates that slightly more than stoichiometric amounts of H_2 and CO_2 are sufficient to convert $NaNO_3$ to $NaHCO_3$ and NH_3. The potential formation of CO from the excess H_2 and CO_2 was meticulously investigated using gas chromatography (GC); however, no CO signal was detected in the GC data (Fig. S2).

A series of experiments were conducted to evaluate the impact of $NaNO_3$ concentration on the yield of $NaHCO_3$. As shown in entries 12–14 of Table 1 and Fig. 2b, the concentration of $NaNO_3$ influences the yield of $NaHCO_3$. Compared to the 4.0 M solution, both higher and lower concentrations result in reduced yields. This indicates that the optimal $NaNO_3$ concentration for maximum $NaHCO_3$ yield is 4.0 M at a total pressure of 25 bar. Interestingly, when the pressure is increased to 50 bar (entry 15, Table 1), complete conversion is achieved with an 8.0 M $NaNO_3$ solution, suggesting that increasing the pressure accelerates the nitrate hydrogenation.

We scaled up the catalytic reaction from a 1 mL scale to a 100 mL scale while maintaining a total pressure of 50 bar (entry 16, Table 1). Complete conversion of $NaNO_3$ to $NaHCO_3$ was observed within 24 hours. Notably, even at a low nitrate concentration (1.18 M), the reaction completed due presumably to the high pressure. The experimental data, although obtained from small-scale reactions, demonstrate that scalable production of $NaHCO_3$ from $NaNO_3$ is possible across a wide concentration range at temperatures below 100 °C.

In addition to $NaHCO_3$, ammonia is also produced through this catalytic process. Gaseous ammonia can be readily isolated from the reaction mixture by passing it through a strong acid trap. By employing sulfuric acid as the trapping agent, ammonia is obtained as an ammonium salt in the form of NH_4HSO_4 (Fig. S2), with yields typically exceeding 92 %. This new catalytic method can produce both $NaHCO_3$ and ammonium complexes, potentially offering an economically viable alternative to the existing Solvay process.

Several experiments, similar to the trial conducted in entry 3 of Table 1, were carried out at 60 °C with different time intervals to elucidate the sequential pathway for nitrate hydrogenation and carbonation. The results from six experiments are depicted in Fig. 3, illustrating changes in yield, pH, and pressure drop over a 24-hour period. After 2 hours of reaction, the pH of the solution increases to 8.8, the pressure drops about 3.5 bar, and the yield of $NaHCO_3$ reaches 24.6 %. Extending the reaction time to 6 hours raises the pH to 9.2, with the yield of $NaHCO_3$ increasing to 67.1 %, albeit with a 9.7 bar pressure drop. Continuing the reaction for 12 hours, the pH slightly increases to 9.4, and the yield of $NaHCO_3$ is 85.6 %, accompanied by a pressure drop of 13 bar. A complete conversion of $NaNO_3$ to $NaHCO_3$ is achieved at 60 °C roughly over 12 hours. After the reaction, the pH of the solution stabilized at about 9.2, and the pressure remained around 12 bar. The yield of $NaHCO_3$ reaches 97.5 %. As depicted in Fig. 3, the $NaNO_3$ conversion increases with prolonged reaction time. However, the pressure experiences a rapid drop at the initial stage, followed by gradual decreases over time. Similarly, the pH of the solution exhibits a rapid increase at the beginning of the reaction, maintaining a relatively constant value thereafter. These results suggest that the nitrate hydrogenation reaction occurs initially, followed by the subsequent carbonation reaction.

3.2. Recyclability of the H_xRuO_2 catalyst

The experimental data described above strongly support the efficacy of the newly developed catalytic process for producing $NaHCO_3$. Now, we turn our attention to evaluating the recyclability of the H_xRuO_2 catalyst, a crucial aspect for constructing an economically viable and sustainable process. Heterogeneous catalysts are typically easy to recover and reuse, playing a pivotal role in reducing the operating costs and carbon footprint of various commercial processes. The used catalyst was separated from the product using deionized water, which dissolves $NaHCO_3$ but not the H_xRuO_2 catalyst. To test the activity of the recovered H_xRuO_2 catalyst, a catalytic reaction was performed under following conditions: 20 mg of catalyst, 4 mmol of $NaNO_3$, 1 mL of water, 20 bar of H_2, 5 bar of CO_2, and a reaction time of 2 hours at 100 °C. The yields of $NaHCO_3$ remain consistently high, exceeding 92 %, throughout the initial 10 cycles, as illustrated in Fig. 4. The sustained activity of the H_xRuO_2 catalyst is quite remarkable, allowing the catalytic process to be employed as an environmentally benign and economically viable route to producing soda ash. The microstructures of the used H_xRuO_2 catalyst consist of an agglomerate of spherical particles with an average diameter of approximately 32 nm, which are quite similar to those of the fresh catalyst (Fig. S3). Additionally, powder XRD

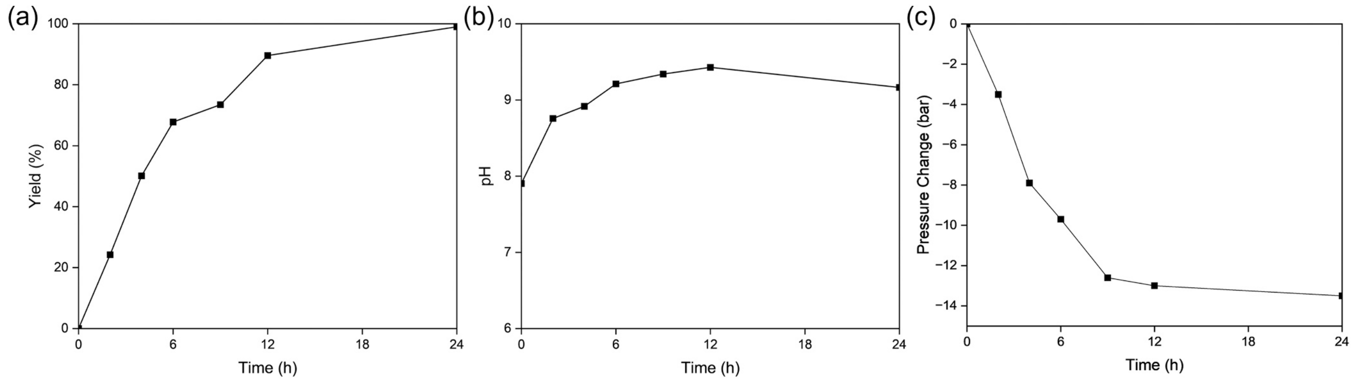

Fig. 3. Progression of nitrate hydrogenation at 60 °C using the H_xRuO_2 catalyst, depicted over 24 hours. The graph illustrates time-dependent data for: (a) the yield of $NaHCO_3$, (b) the pH of the solution after the reaction, and (c) the change in pressure within the reaction vessel. Experimental setup included 20 mg of catalyst, 4 mmol of $NaNO_3$, 1 mL of water, and gas pressures of 20 bar H_2 and 5 bar CO_2.

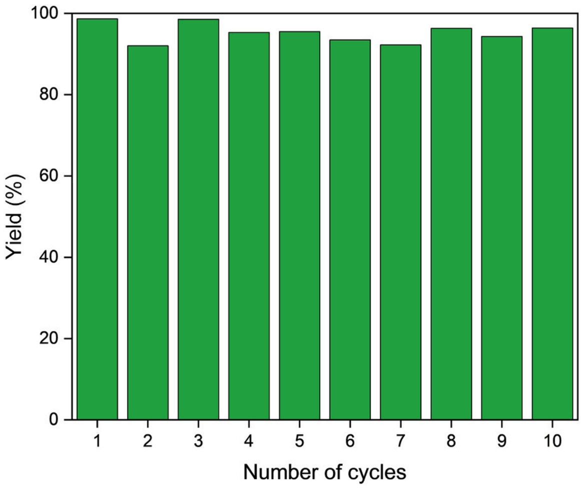

Fig. 4. Assessing the recyclability of the H_xRuO_2 catalyst. This graph shows the yields of $NaHCO_3$ obtained from each of ten consecutive reaction cycles performed under identical conditions. Reaction conditions: 20 mg of catalyst, 4 mmol of $NaNO_3$, 1 mL of water, 20 bar H_2, 5 bar CO_2 at 100 °C for 3 hours.

data of the used H_xRuO_2 catalyst match well with those of pure H_xRuO_2 and do not show any indications of decomposed products such as Ru and RuO_2 (Fig. S3) [29].

3.3. Techno economic analysis and life cycle assessment

To evaluate technical performance and economic feasibility, a techno economic analysis was conducted for the conversion of $NaNO_3$ to Na_2CO_3. Fig. 5a illustrates a process flow diagram of this conversion process, which consists of four sections designed for continuous operation and developed using Aspen Plus V12. The four sections include: Conversion of $NaNO_3$ (Section 1), Calcination of $NaHCO_3$ (Section 2), Separation of NH_4HCO_3 (Section 3), and Crystallization of Na_2CO_3 (Section 4). For the base case scenario, operating conditions and reaction specifications were established based on the experimental data provided in entry 6 of Table 1.

In Section 1, the process begins with selective hydrogenation of nitrate to ammonia, followed by the formation of $NaHCO_3$ and NH_4HCO_3. $NaHCO_3$ can be separated as a solid from NH_4HCO_3 due to a significant difference in their solubility at around room temperature (Fig. S4). Unreacted H_2 and CO_2 gases are recycled. The catalyst is reused after filtering the RX1 outlet stream. In the calcination step (Section 2), $NaHCO_3$ is converted into Na_2CO_3 by releasing CO_2, while NH_4HCO_3 decomposes into NH_3, CO_2, and H_2O. The solid Na_2CO_3 is separated from the gaseous stream in SEP2. Subsequently, NH_4HCO_3 is isolated as a solid, and the remaining CO_2 and H_2O are recycled (Section 3). In the crystallization stage (Section 4), sodium carbonate is isolated in the hydrate form ($Na_2CO_3{\cdot}xH_2O$), which is transformed into anhydrous dense soda ash (Na_2CO_3) during the drying step.

The breakdowns of capital expenditure (CAPEX) and operating expenditure (OPEX) for the catalytic conversion process are illustrated in Fig. 5b, representing the base case scenario. The specific CAPEX and OPEX data used are detailed in Table S2. In the CAPEX breakdown (far left graph), the compressor (COM) section is the predominant contributor, accounting for approximately 57 %. This is primarily due to the gas compression of H_2 and CO_2. Fig. 5b displays two OPEX breakdowns: one for utilities (middle graph) and the other for feedstock (far right graph). The feedstock costs constitute 96.2 % of the total OPEX, with the remaining 4.3 % attributed to utility expenses. The two primary contributors in the feedstock section are the costs of $NaNO_3$ and H_2, contributing 57 % and 40 %, respectively.

The base case simulation estimates that the catalytic process produces 184 kilotons per year of Na_2CO_3 and 241 kilotons per year of NH_4HCO_3. Additionally, revenue is generated from selling carbon credits derived from the emitted CO_2 (Fig. S5). Profits from NH_4HCO_3 and carbon credits amount to $147 million per year, representing 40 % of the total revenue (Fig. S5). The major advantage of the Solvay process is its use of inexpensive raw materials such as brine (NaCl) and limestone ($CaCO_3$). However, the process requires a significant amount of NH_3 to initiate and involves the calcination of $CaCO_3$ to CaO at 850 °C. In contrast, the catalytic process can reduce steam consumption by approximately 54 % (Table S3).

As shown in Fig. 5b, feedstock costs have the largest impact on the catalytic process. We assumed that green hydrogen, produced from renewable energy, could be used as a raw material. The minimum selling price (MSP) of Na_2CO_3, estimated from the base case, is $1.27/kg (Fig. 5c). Although the MSP under base case conditions is higher than that of the Solvay process, there are significant opportunities to reduce the MSP by adjusting the prices of $NaNO_3$ and H_2. We varied these prices to evaluate their impact on the MSP, as illustrated in Fig. 5c. The details of base and optimal conditions are provided in Table S4 and Table S5. Under optimal conditions, the MSP is estimated to be $0.17/kg, which is lower than the $0.31/kg price of Na_2CO_3 produced by the Solvay process.

We conducted a life cycle assessment to evaluate the potential environmental impacts of the catalytic process. The cradle-to-gate approach was used, with a functional unit of 1 kg of soda ash (Na_2CO_3) production. Fig. 5d illustrates the global warming impact (GWI) results for the Solvay process, the catalytic process under base conditions, and the catalytic process under optimal conditions. Compared to the Solvay process, the catalytic process under base

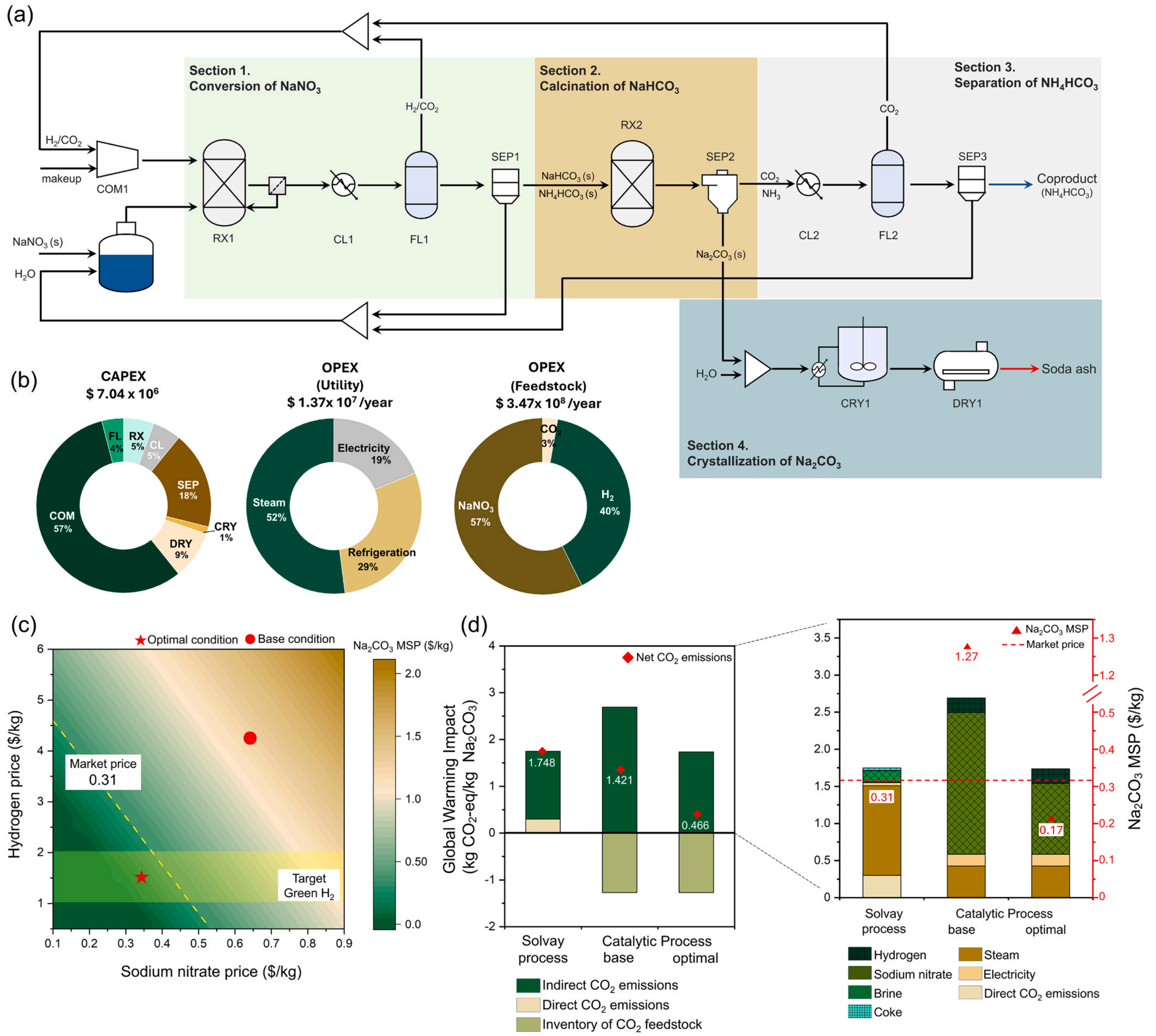

Fig. 5. Techno economic analysis and life cycle assessment of the conversion of $NaNO_3$ to soda ash (Na_2CO_3). (a) Simplified process flow diagram of the catalytic process, consisting of four sections. Abbreviations are as follows: COM, compressor; RX, reactor; FL, flash; SEP, separator; CL, chiller; CRY, crystallization; DRY, dryer. (b) Breakdown of CAPEX, OPEX (Utility), and OPEX (Feedstock) for the catalytic process. Detailed data for these breakdowns are provided in Table S2 and Table S3. (c) Minimum selling price (MSP) of Na_2CO_3 estimated based on the prices of $NaNO_3$ and H_2. The yellow dashed line represents the market price, and the white box indicates the prices for target green H_2 [30]. The red circle and star symbols represent the base and optimal scenario conditions, respectively. Detailed data for base and optimal conditions are provided in Table S4 and Table S5. (d) Comparison of global warming impact (GWI) results for the Solvay process, the catalytic process under base conditions, and the catalytic process under optimal conditions. We assumed that the MSP of soda ash produced by the Solvay process is equal to the market price. Red diamonds and red triangles denote net CO_2 emissions and MSP of Na_2CO_3, respectively.

conditions can reduce net CO_2 emissions by 19 %. When optimal conditions are applied, net CO_2 emissions are significantly reduced by 73 %, improving the GWI factor.

To achieve both economic viability and environmental sustainability, two key factors are required: low-cost green hydrogen and an inexpensive $NaNO_3$ supply. Additionally, reducing CO_2 emissions from $NaNO_3$ production can significantly improve both the MSP and GWI values. Under optimal conditions, the MSP is \$0.17/kg and the GWI is 0.466 kg CO_2-eq/kg. Detailed factors for the techno economic analysis (TEA) and life cycle assessment (LCA) are provided in the Supplementary Information.

3.4. *Catalytic synthesis of sodium bicarbonate from sodium chloride*

The catalytic process described above demonstrates proof of concept for producing sodium bicarbonate ($NaHCO_3$) with negligible CO_2 emissions. However, the starting material sodium nitrate ($NaNO_3$) is both limited and expensive. By utilizing abundant salt brine (NaCl) as a sodium source, similar to the Solvay process, we can enhance the feasibility of this catalytic approach. We thus evaluated the suitability of NaCl as a precursor for $NaHCO_3$ production by conducting catalytic reactions at 60 °C for 24 hours under a total pressure of 50 bar (40 bar of H_2 and 10 bar of CO_2) using 20 mg of catalyst, 4 mmol of NaCl, and 4 mL of 1 M HNO_3. As shown in Figure S6, $NaHCO_3$ was successfully formed alongside ammonium chloride (NH_4Cl), confirming the applicability of our catalytic technology to salt brine.

Notably, this process can also utilize nitric acid waste from industrial manufacturing, salt brine, and CO_2 emissions from combustion sources. This versatility could significantly reduce the overall costs of our catalytic method and enhance carbon neutrality in the soda ash and limestone industries. The full potential of our catalytic approach may be realized by pairing it with green electricity for hydrogen production, leading to a more sustainable supply of sodium nitrate.

4. Conclusions

We have demonstrated proof of concept for a new catalytic process that might replace the current Solvay process, producing soda ash (Na_2CO_3) in a more eco-friendly and sustainable manner. This catalytic strategy utilizes $NaNO_3$, CO_2, and H_2 as starting raw materials. Unlike the Solvay process, our catalytic process not only avoids CO_2 emissions but also does not produce any byproducts that could cause environmental issues. Our laboratory-scale experiments demonstrated that a short reaction time and mild reaction temperature are sufficient for the complete conversion of $NaNO_3$ into $NaHCO_3$ and NH_4HCO_3, which is advantageous for scaling up production. Additionally, the stability of the H_xRuO_2 catalyst offers a significant industrial advantage, highlighting the robustness of the catalytic process. An important challenge in scaling this newly discovered catalytic process for industrial use is the cost of $NaNO_3$ and H_2. However, this cost can be partially offset by the value of the ammonia compounds produced from nitrate hydrogenation and by utilizing hydrogen generated from surplus renewable electricity. Furthermore, the use of salt brine and nitric acid waste as starting reagents enhances the economic viability of this catalytic approach.

The proposed technology, based on the catalytic reaction, offers a novel route for reducing the substantial CO_2 emissions associated with the calcination of $CaCO_3$ in the Solvay process. More importantly, this catalytic approach not only provides an innovative, breakthrough, and eco-friendly soda ash production process but also represents a significant step forward toward the global carbon neutrality target. Consequently, our catalytic process, which does not use $CaCO_3$, can be an alternative to the current Solvay process.

CRediT authorship contribution statement

Na Jonggeol: Writing – original draft, Supervision. **Hur Nam Hwi:** Writing – review & editing, Writing – original draft, Supervision, Methodology, Conceptualization. **Yang Hee Jung:** Formal analysis. **Chung Youlim:** Writing – original draft, Investigation. **Park Hee Sun:** Writing – original draft, Methodology, Investigation, Data curation. **Kim Jae Yeon:** Investigation, Formal analysis.

Declaration of Competing Interest

The authors declare that they have no known competing financial interests or personal relationships that could have appeared to influence the work reported in this paper.

Acknowledgements

The work at SU (N.H.H) was supported by the National Research Foundation (NRF) funded by the Korean Government (MSIT) (grant no. RS-2024-00422888). The work at EWU (J.N) was supported by the National Research Foundation (NRF) funded by the Korean Government (MSIT) (RS-2024-00431568).

Appendix A. Supporting information

Supplementary data associated with this article can be found in the online version at doi:10.1016/j.jcou.2025.103060.

Data Availability

No data was used for the research described in the article.

References

[1] U.S. Geological Survey, Mineral commodity summaries, ⟨https://pubs.usgs.gov/periodicals/mcs2024/mcs2024-soda-ash.pdf⟩ (Accessed 29 July 2024).

[2] A. Scott, Can synthetic soda ash survive? CEN 101 (2023) 20–22.

[3] H. Cui, WO Pat., 2012129962A2, 2012.

[4] U.S. Environmental Protection Agency, Technical support document for the soda ash manufacturing sector: Proposed rule for mandatory reporting of greenhouse gases, 2009, ⟨https://nepis.epa.gov/Exe/ZyPURL.cgi?Dockey=P1009F3C.txt⟩.

[5] G. Steinhauser, Cleaner production in the Solvay process: general strategies and recent developments, J. Clean. Prod. 16 (2008) 833–841.

[6] M. Rumayor, A. Dominguez-Ramos, A. Irabien, Toward the decarbonization of hard-to-abate sectors: a case study of the soda ash production, ACS Sustain. Chem. Eng. 8 (2020) 11956–11966.

[7] M. Simoni, T. Hanein, C.L. Woo, J. Provis, H. Kinoshita, Effect of impurities on the decarbonization of calcium carbonate using aqueous sodium hydroxide, ACS Sustain. Chem. Eng. 10 (2022) 11913–11925.

[8] H. Song, C.A. Fernández, H. Choi, P.-W. Huang, J. Oh, M.C. Hatzell, Integrated carbon capture and CO production from bicarbonates through bipolar membrane electrolysis, Energy Environ. Sci. 17 (2024) 3570–3579.

[9] S. Ghaffari, M.F. Gutierrez, A. Seidel-Morgenstern, H. Lorenz, P. Schulze, Sodium hydroxide-based CO_2 direct air capture for soda ash production-Fundamentals for process engineering, Ind. Eng. Chem. Res. 62 (2023) 7566–7579.

[10] T. Setayeshmanesh, M.M. Parivazh, M. Abbasi, S. Osfouri, M.J. Dianat, M. Akrami, Reducing the environmental impacts of desalination reject brine using modified Solvay process based on calcium oxide, Sustainability 14 (2022) 2298.

[11] J. Su, M. Lu, H. Lin, High yield production of formate by hydrogenating CO_2 derived ammonium carbamate/carbonate at room temperature, Green. Chem. 17 (2015) 2769–2773.

[12] J.H. Lee, J.H. Lee, I.K. Park, C.H. Lee, Techno-economic and environmental evaluation of CO_2 mineralization technology based on bench-scale experiments, J. CO_2 Util. 26 (2018) 522–536.

[13] J.H. Lee, D.W. Lee, C. Kwak, K. Kang, J.H. Lee, Technoeconomic and environmental evaluation of sodium bicarbonate production using CO_2 from flue gas of a coal-fired power plant, Ind. Eng. Chem. Res. 58 (2019) 15533–15541.

[14] L. Rincón, C. Ruiz, R.R. Contreras, J. Almarza, Study of the NaOH(s)–CO_2(g) reaction creating value for industry: green natrite production, energy, and its potential in different sustainable scenarios, Environ. Sci.: Adv. 2 (2023) 957–966.

[15] Q. Wang, Z. Li, A modified Solvay process with low-temperature calcination of $NaHCO_3$ using monoethanolamine: Solubility determination and thermodynamic modeling, AIChE J. 65 (2019) e16701.

[16] Y. Wu, H. Xie, T. Liu, Y. Wang, F. Wang, X. Gao, B. Liang, Soda ash production with low energy consumption using proton cycled membrane electrolysis, Ind. Eng. Chem. Res. 58 (2019) 3450–3458.

[17] M. Forster, Investigations for the environmentally friendly production of Na_2CO_3 and HCl from exhaust CO_2, NaCl and H_2O, J. Clean. Prod. 23 (2012) 195–208.

[18] S. Seki, The ammonium chloride and soda ash dual manufacturing process in Japan, UN, 1969.

[19] T. Hanein, M. Simoni, C.L. Woo, J.L. Provis, H. Kinoshita, Decarbonisation of calcium carbonate at atmospheric temperatures and pressures, with simultaneous CO_2 capture, through production of sodium carbonate, Energy Environ. Sci. 14 (2021) 6595–6604.

[20] G.-F. Chen, Y. Yuan, H. Jiang, S.-Y. Ren, L.-X. Ding, L. Ma, T. Wu, J. Lu, H. Wang, Electrochemical reduction of nitrate to ammonia via direct eight-electron transfer using a copper–molecular solid catalyst, Nat. Energy 5 (2020) 605–613.

[21] P. Ramadhany, T. Trần-Phú, J.A. Yuwono, Z. Ma, C. Han, T.K.A. Nguyen, J. Leverett, P. Kumar, R.K. Hocking, A. Tricoli, A.N. Simonov, R. Amal, R. Daiyan, Triggering C-N coupling on metal oxide nanocomposite for the electrochemical reduction of CO_2 and NO_x^- to formamide, Adv. Energy Mater. 14 (2024) 2401786.

[22] J.E. Kim, J.H. Jang, K.M. Lee, M. Balamurugan, Y.I. Jo, M.Y. Lee, S. Choi, S.W. Im, K.T. Nam, Electrochemical synthesis of glycine from oxalic acid and nitrate, Angew. Chem. Int. Ed. 60 (2021) 21943–21951.

[23] L. Wei, D.-J. Liu, B.A. Rosales, J.W. Evans, J. Vela, Mild and selective hydrogenation of nitrate to ammonia in the absence of noble metals, ACS Catal. 10 (2020) 3618–3628.

[24] S. Zhang, J. Wu, M. Zheng, X. Jin, Z. Shen, Z. Li, Y. Wang, Q. Wang, X. Wang, H. Wei, J. Zhang, P. Wang, S. Zhang, L. Yu, L. Dong, Q. Zhu, H. Zhang, J. Lu, Fe/Cu diatomic catalysts for electrochemical nitrate reduction to ammonia, Nat. Commun. 14 (2023) 3634.

[25] Q. Gou, Y. Mao, S. Lv, F. Gou, Y. Jiang, W. Shen, M. Li, Y. Wang, R. He, Enhancing nitrate reduction to ammonia by synergistic and interface coupling effects of binary metal sites, Appl. Catal. B 348 (2024) 123810.

[26] K. Yu, H. Wang, W. Yu, S. Li, X. Zhang, Z. Bian, Resource utilization of carbon dioxide and nitrate to produce value-added organonitrogen compounds through an electrochemical approach, Appl. Catal., B 341 (2024) 123292.

[27] W.C. Elias, K.N. Heck, S. Guo, S. Yazdi, C. Ayala-Orozco, S. Grossweiler, J. B. Domingos, E. Ringe, M.S. Wong, Indium-decorated Pd nanocubes degrade nitrate anions rapidly, Appl. Catal., B 276 (2020) 119048.

[28] K. Flores, D. Varda, N. Hald, G.A. Cerrón-Calle, M.A. Roldan, S. Garcia- Segura, Engineering copper supported mixed manganese oxides as selective bimetallic

electrocatalyst for nitrate to ammonia conversion at environmentally relevant concentrations, Appl. Catal., B (2024) 124682.

[29] H.J. Yang, M. Redington, D.P. Miller, E. Zurek, M. Kim, C.-S. Yoo, S.Y. Lim, H. Cheong, S.-A. Chae, D. Ahn, N.H. Hur, New monoclinic ruthenium dioxide with highly selective hydrogenation activity, Catal. Sci. Technol. 12 (2022) 6556–6565.

[30] W.D. Seider, J.D. Seader, D.R. Lewin, Process Design Principles: Synthesis, Analysis, and Evaluation, John Wiley & Sons, Inc, New York, 1999.

[31] A.-M. Cormos, C.-C. Cormos, P.Ş. Agachi, Making soda ash manufacture more sustainable. A Modeling Study using ASPEN Plus, Elsevier, Amsterdam, 2007.

[32] H.C.M. Hungaro Yoshi, A.B. Silva, M. De Souza, S.H. Bernardo De Faria, A. Bernardo, L. Bonfim-Rocha, Multi-criteria assessment of sodium bicarbonate optimized production through CO_2 utilization strategies, J. Clean. Prod. 349 (2022) 131419.

[33] F. Frieden, J. Leker, Future costs of hydrogen: a quantitative review, Sustain. Energy Fuels 8 (2024) 1806–1822.

[34] G. Glenk, S. Reichelstein, Economics of converting renewable power to hydrogen, Nat. Energy 4 (2019) 216–222.

[35] Business Analytiq., ⟨https://businessanalytiq.com/procurementanalytics/index/sodium-nitrate-price-index/⟩ (Accessed July 25, 2024).

[36] K.H. Büchel, H.-H. Moretto, D. Werner, Industrial Inorganic Chemistry, John Wiley & Sons, Inc, New York, 2008.

[37] S. Wei, R. Sacchi, A. Tukker, S. Suh, B. Steubing, Future environmental impacts of global hydrogen production, Energy Environ. Sci. 17 (2024) 2157–2172.

[38] H.S. Park, H.J. Yang, S. Kim, S.T. Hong, N.H. Hur, Recovery of valuable metals from spent lithium-ion batteries through an ecofriendly catalytic approach, J. Power Sources 594 (2024) 234024.